



Functional characterization and expression analysis of c-type and g-like-type lysozymes in yellowtail clownfish (*Amphiprion clarkii*)

Gaeun Kim¹, Hanchang Sohn^{1,2}, WKM Omeka¹, Chaehyeon Lim¹, Don Anushka Sandaruwan Elvitigala³, Jehee Lee^{1,2,*}

¹ Department of Marine Life Sciences & Fish Vaccine Research Center, Jeju National University, Jeju 63243, Korea

² Marine Science Institute, Jeju National University, Jeju 63333, Korea

³ Department of Basic Sciences and Social Science for Nursing, Faculty of Nursing, University of Colombo, Thalapatpitiya, Nugegoda 10250, Sri Lanka

Abstract

Lysozymes are well-known antibacterial enzymes that mainly target the peptidoglycan layer of the bacterial cell wall. Animal lysozymes are mainly categorized as g-type, c-type, and i-type based on protein sequence and structural differences. In this study, c-type (AcLysC) and g-like-type (AcLysG-like) lysozymes from *Amphiprion clarkii* were characterized *in silico* via expressional and functional approaches. According to *in silico* analysis, open reading frames of AcLysC and AcLysG-like were 429 bp and 570 bp, respectively, encoding the corresponding polypeptide chains with 142 and 189 amino acids. Elevated expression levels of AcLysC and AcLysG-like were observed in the liver and the heart tissues, respectively, as evidenced by quantitative real-time polymerase chain reaction assays. AcLysC and AcLysG-like transcript levels were upregulated in gills, head kidney, and blood cells following experimental immune stimulation. Recombinant AcLysC exhibited potent lytic activity against *Vibrio anguillarum*, whereas recombinant AcLysG-like showed remarkable antibacterial activity against *Vibrio harveyi* and *Streptococcus parauberis*, which was further evidenced by scanning electron microscopic imaging of destructed bacterial cell walls. The findings of this study collectively suggest the potential roles of AcLysC and AcLysG-like in host immune defense.

Keywords: *Amphiprion clarkii*, c-type lysozyme, g-like-type lysozyme, Immune stimulation, Antibacterial activity

Introduction

Innate immunity is an important defense system in fish species, dealing with a broad spectrum of pathogens. Lysozymes are well-known players in the innate immune mechanisms of fish,

performing diverse functional roles, including antimicrobial, immunomodulatory, anti-inflammatory, and antitumor activities in living organisms (Kokoshis et al., 1978; Lee-Huang et al., 1999; Nilojan et al., 2017; Sava et al., 1988). They are distributed in a wide range of tissues and body fluids, such as mucus, lymph, and

Received: Jun 9, 2022 Revised: Sep 7, 2022 Accepted: Jan 10, 2023

*Corresponding author: Jehee Lee

Department of Marine Life Sciences & Fish Vaccine Research Center, Jeju National University, Jeju 63243, Korea

Tel: +82-64-754-3472, Fax: +82-64-784-0106, E-mail: jehee@jejunu.ac.kr

This is an Open Access article distributed under the terms of the Creative Commons Attribution Non-Commercial License (<http://creativecommons.org/licenses/by-nc/4.0/>) which permits unrestricted non-commercial use, distribution, and reproduction in any medium, provided the original work is properly cited.

Copyright © 2023 The Korean Society of Fisheries and Aquatic Science

plasma of both freshwater and marine fish (Saurabh & Sahoo, 2008). Lysozyme activity and expression are reportedly modulated under different abiotic (degree of stress, pH, water temperature, content of pollutants, and environmental salinity) and biotic (sexual maturity stages, sex, age, and size) conditions (Saurabh & Sahoo, 2008). Lysozymes protect organisms from microbial infections by destroying the bacterial cell wall by hydrolyzing the β -1, 4-glycosidic bond in the peptidoglycan layer (Umasuthan et al., 2013); therefore, lysozymes exert a powerful antibacterial function against gram-positive bacteria by solubilizing the peptidoglycan layer. However, gram-negative bacteria are resistant to cationic antimicrobial peptides, as their peptidoglycan layer is less vulnerable to hydrolysis by lysozymes (Hancock & Scott, 2000).

There are three types of lysozymes: a-type (animal), p-type (plant), and m-type (microbial) (Li et al., 2018). Depending on the amino acid sequence and their chemical and biological properties, animal-type lysozymes are further divided into three subclasses: c-type (chicken), g-type (goose), and i-type (invertebrate) (Pridgeon et al., 2013). The c- and g-type lysozymes were discovered in both invertebrates and vertebrates, whereas i-type lysozymes were identified only in invertebrates. Generally, the secondary structure of lysozymes comprises four alpha helices and five beta strands (Prilusky et al., 2011). All three types of lysozymes share a similar tertiary structure but have low homogeneity in the underlying structure (Li et al., 2019). The c-type lysozyme was first extracted from chicken egg white, and the g-type lysozyme was identified in egg white from Embden goose (Xie et al., 2019). Furthermore, c- and g-type lysozymes have been previously reported in various marine animals, such as Yangtze sturgeon (*Acipenser dabryanus*) (Zhang et al., 2018), longtooth grouper (*Epinephelus bruneus*) (Harikrishnan et al., 2011), orange-spotted grouper (*Epinephelus coioides*) (Wei et al., 2012), Manila clam (*Ruditapes philippinarum*) (Wei et al., 2018), Japanese flounder (*Paralichthys olivaceus*) (Hikima et al., 2001), seahorse (*Hippocampus abdominalis*) (Ko et al., 2016), and turbot (*Scophthalmus maximus*) (Zhao et al., 2011). However, very few reports reveal the *in vitro* antibacterial activity of c-type lysozyme and g-type-like lysozyme in ornamental fish (Smith et al., 2012).

As the demand for ornamental aquaculture grows and the aquarium trade increases, many studies have focused on the growth and immune systems of ornamental fish to enable more systemic aquacultural production (Avella et al., 2007). Yellowtail clownfish (*Amphiprion clarkii*) is one of the most frequently demanded members of Amphiprioninae in aquarium trade markets. It is found in coral reefs or shallow lagoons in the Indian Ocean,

Pacific Ocean, and the Red Sea, where the water temperature is approximately 22 °C–29 °C (Yanagisawa & Ochi, 1986). Moreover, it inhabits the ocean around Jeju Island in South Korea. Nearly 90% of all marine ornamental species are captured by fishing. To develop sustainable ornamental fish aquaculture, it is essential to implement a proper breeding system and reduce lethal infections such as vibriosis, edwardsiellosis, and lymphocystis. Moreover, clownfish are now emerging as potential model organisms of interest for developmental biology, ecology, and evolutionary science (Roux et al., 2020). Therefore, understanding the innate immune mechanisms in *A. clarkii* can help develop useful strategies for preventing diseases in ornamental fish aquaculture. In this study, two lysozymes, c-type lysozyme (AcLysC) and g-like-type lysozyme (AcLysG-like) were identified and characterized at the molecular level to elucidate their functional roles in *A. clarkii*.

Materials and Methods

Experimental animals

Healthy *A. clarkii* with an average body weight of 20 g and an average body length of 10 cm were obtained from the Choryang Aquarium, Busan, Korea. The fish were acclimated in laboratory aquarium tanks (300 L) at a constant temperature of 28 °C and 32 PSU (practical salinity unit) for one week prior to experiments. During acclimatization, fish were fed a commercial fish feed twice daily and deprived of feed two days prior to the experiment.

Tissue collection for *Amphiprion clarkii* transcriptome and tissue-specific mRNA expression analyses

Tissues were collected from *A. clarkii* (n = 5) to perform the transcriptome and tissue-specific expression analyses of AcLysC and AcLysG-like. First, conventional anesthetics (MS-222; 40 mg/L) were used to anesthetize healthy *A. clarkii*. Then, the fish were dissected, and the head kidney, intestine, heart, liver, brain, gill, spleen, kidney, muscle, skin, and stomach tissues were collected. Blood was also sampled using sterile syringes coated with heparin sodium salt (Sigma-Aldrich, St. Louis, MO, USA). Peripheral blood cells were immediately harvested by centrifugation at 3,000×g for 10 min at 4 °C. All tissues were immediately snap-frozen in liquid nitrogen and stored at –80 °C until RNA isolation.

Immune stimulation

To evaluate the modulation of AcLysC and AcLysG-like against immune stimulation, two chemical stimulants and a live bacterial pathogen were used in time-course experiments. Briefly, the

acclimatized *A. clarkii* were randomly divided into four groups (each group including four animals). Fish of three groups constituting the test groups for this experiment were administered a single intraperitoneal injection of either lipopolysaccharide (LPS; 2.5 µg/g, Sigma-Aldrich), polyinosinic: polycytidylic acid (Poly I:C; 2.5 µg/g, Sigma-Aldrich), or *Vibrio harveyi* (1×10^3 CFU/µL) suspended in 100 µL of phosphate-buffered saline (PBS). Fish in the control group were injected with 100 µL of PBS. Tissues were collected at 0, 6, 12, 24, 48, and 72 h post-injection (p.i.). All tissues were snap-frozen in liquid nitrogen and stored at -80°C until RNA isolation. All experimental procedures involved in this study were reviewed and approved by the Animal Care and Use Committee of the Jeju National University.

Establishment of transcriptome database, RNA extraction, and cDNA synthesis

To prepare the transcriptome library, total RNA was extracted from collected tissues. RNA extraction was performed using TRIzol (Invitrogen, Waltham, MA, USA), followed by clean-up with a RNeasy spin column (Qiagen, Hilden, Germany) according to the manufacturer's instructions. The extracted RNA was assessed for quality, quantified using a 2100 Expert Bioanalyzer (Agilent Technologies, Santa Clara, CA, USA), and sequenced at Insilicogen (Yongin, Korea). The transcriptome database of *A. clarkii* was constructed using the Illumina NovaSeq6000 and assembled *de novo* at Insilicogen.

For expression analysis (tissue distribution, $n = 5$; immune challenge, $n = 4$), total RNA was extracted, and the purity of the isolated RNA was examined with 1.5% agarose gel electrophoresis. The concentration was determined based on the absorbance at 260 nm and 280 nm, measured using a µDrop Plate (Thermo Scientific, Waltham, MA, USA). First-strand cDNA was synthesized in a 20 µL reaction mixture containing a pool of RNA (2.5 µg of RNA from tissue distribution samples, 2.0 µg of RNA from immune challenge samples) with PrimeScript™ II 1st strand cDNA Synthesis Kit (TaKaRa, Shiga, Japan) according to the recommended procedures. The synthesized cDNA was diluted 40-fold in nuclease-free water and stored in a freezer at -80°C until further use.

In silico profiling of AcLysC and AcLysG-like

The cDNA sequences of *AcLysC* (MK835689) and *AcLysG-like* (MW199185) were identified from the established *A. clarkii* transcriptomic database using the NCBI BLAST tool based on the sequence alignments with respective lysozyme homologs in NCBI-GenBank database. The open reading frame sequences

(ORFs) of *AcLysC* and *AcLysG-like* were obtained using the NCBI ORF Finder (<https://www.ncbi.nlm.nih.gov/orffinder/>). Then, the corresponding amino acid sequences were verified using the NCBI BLAST program (<https://blast.ncbi.nlm.nih.gov/Blast.cgi>). Signal peptides of *AcLysC* and *AcLysG-like* were analyzed using the SignalP 5.0 online tool (<http://www.cbs.dtu.dk/services/SignalP/>). The domain organization and signature motifs in the *AcLysC* and *AcLysG-like* amino acid sequences were identified using the NCBI conserved domain database (<https://www.ncbi.nlm.nih.gov/Structure/cdd/wrpsb.cgi>) and Motif Scan (https://myhits.sib.swiss/cgi-bin/motif_scan) online server. Moreover, multiple sequence alignments of deduced *AcLysC* and *AcLysG-like* protein sequences with corresponding homologs were performed using the CLC Main Workbench (version 8.0) software. A phylogenetic tree comprising different homologous sequences of *AcLysC* and *AcLysG-like* was constructed using the neighbor-joining method embedded in the MEGA 6.0 software. The reliance value for the phylogenetic tree was obtained by replicating bootstrap trials 5,000 times.

Transcriptional analysis of AcLysC and AcLysG-like by quantitative real-time polymerase chain reaction (qPCR)

Quantitative real-time polymerase chain reaction (qPCR) was carried out using a Thermal Cycler Dice™ TP 950 (TaKaRa) in a 10 µL reaction volume containing 3 µL of diluted cDNA template, 5 µL of $2 \times$ Ex Taq™ SYBR premix (TaKaRa), 0.4 µL each of the forward and reverse primers (10 pmol/µL), and 1.2 µL of PCR-grade H₂O (Table 1). The qPCR thermal cycles included one cycle of 95°C for 10 s, followed by 45 cycles of 95°C for 5 s, 58°C for 10 s, 72°C for 20 s, and a final single cycle of 95°C for 15 s, 60°C for 30 s, and 95°C for 15 s. Each assay was conducted in triplicates. The $2^{-\Delta\Delta Ct}$ method was used to calculate the relative expression of each gene (Livak & Schmittgen, 2001). Elongation factor 1-beta (*Ef1β*) of *A. clarkii* (MN970208.1) was used as the internal control gene for all qPCR assays. Furthermore, mRNA expression levels of the immune-stimulated group were normalized to those of relevant PBS-injected control at each time point. The obtained results were represented as mean \pm SD. Expression level at 0 h (uninjected control) was used as the basal level reference for the expression profiles of immune-stimulated fish. An independent, two-tailed *t*-test was carried out to identify the statistically significant fold expression values of immune-stimulated animals at $p < 0.05$ and $p < 0.01$.

Table 1. Details of the primers used in this study

Primer name	Sequence 5'-3'	Description
AcLysC cloning forward	GAGAGAccatggggcCTGGAGCGCTGTGCATGG	Tm 59.6°C, 378 bp, NcoI
AcLysC cloning reverse	GAGAGAgaattcCTAAAGTCCACATCCGGCTATGTGAACT	Tm 59.5°C, 378 bp, EcoRI
AcLysC qPCR forward	AGGGATGCTGGGATGGATGGTTA	Tm 60°C, 134 bp
AcLysC qPCR reverse	TGAAAGATGCCGTAGTCGGTGGAT	Tm 60°C, 134 bp
AcLysG-like cloning forward	GAGAGAcatatgATGGGTTATGGAACATCATGCGTGT	Tm 59.1°C, 570 bp, NdeI
AcLysG-like cloning reverse	GAGAGAgaattcTAAAAGCCACCGCTAGTTTTGTACCAC	Tm 59.3°C, 570 bp, EcoRI
AcLysG-like qPCR forward	ATCACACATGATGGCAGAGACGGATG	Tm 60°C, 122 bp
AcLysG-like qPCR reverse	ACTCTCTGGAGATGATGGCAGCAATG	Tm 60°C, 122 bp
Ef-1 β qPCR reference gene forward	AGAACAGTCTGCCAGGTGTGAAGAAG	Tm 60°C, 132 bp
Ef-1 β qPCR reference gene reverse	TGTCAGAGCCAAACAGGTCTGATGT	Tm 60°C, 132 bp

qPCR, quantitative real-time polymerase chain reaction.

Cloning, recombinant protein expression and purification

Primer pairs were designed for PCR amplification of the ORFs of *AcLysC* and *AcLysG*-like with suitable restriction sites (Table 1) for cloning into the expression vector pMAL-c5X (NEB, Ipswich, MA, USA). The coding sequence was amplified from cDNA using Ex Taq polymerase (TaKaRa). Amplified PCR products and the pMAL-c5X vector were separately digested with respective restriction enzymes. Digested ORFs were separately ligated into the pMAL-c5X vector using DNA Ligation Mighty Mix (TaKaRa). The recombinant expression vector for each gene was transformed into *Escherichia coli* DH5 α cells. Successful transformants were identified by colony PCR and confirmed by sequencing (Macrogen, Seoul, Korea). Sequence-confirmed colonies were subjected to plasmid extraction using the AccuPrep[®] Plasmid MiniPrep DNA Extraction Kit as per the vendor's protocol (Bioneer, Daejeon, Korea).

The recombinant *AcLysC* and *AcLysG*-like plasmids were transformed into *E. coli* ER2523 cells. Recombinant bacterial cells were cultured in 500 mL Luria-Bertani broth supplemented with 2.0 g of glucose and 100 μ g/mL ampicillin. Cells were grown at 37°C in a shaking incubator (200 rpm) until the optical density (OD) at 600 nm reached 0.7. At the optimal OD, protein expression was induced by adding a final concentration of 0.25 mM isopropyl- β -thiogalactopyranoside (IPTG) and incubating for 8 h at 25°C. Bacterial cultures were then cooled on ice for 30 min. Subsequently, bacteria were harvested by centrifugation at 4,000 \times g for 30 min at 4°C, and the obtained cell pellets were resuspended in 25 mL of column buffer (20 mM Tris-HCl, pH 7.4, 200 mM NaCl, 0.5 M EDTA). The fusion protein with maltose-binding protein (MBP) was purified by amylose affinity chromatography, as described

in the pMAL protein fusion and purification manual (NEB). All subsequent purification steps were performed on ice or at 4°C. The purified protein concentration was determined by the Bradford protein assay (Bio-Rad, Hercules, CA, USA). The quality and quantity of the recombinant proteins at different purification steps were evaluated by 12% sodium dodecyl sulfate-polyacrylamide electrophoresis (SDS-PAGE) under reducing conditions.

Antimicrobial activity of *AcLysC* and *AcLysG*-like

The antibacterial activity of *AcLysC* and *AcLysG*-like recombinant proteins were analyzed against four gram-negative (*Edwardsiella tarda*, *Photobacterium damsela* subsp. *piscicida*, *Vibrio anguillarum*, and *V. harveyi*) and two gram-positive (*Micrococcus luteus* and *Streptococcus parauberis*) using a previously reported turbidimetric assay (Xue et al., 2004) in a buffer system at pH 4.0 (sodium acetate–acetic acid, 50 mM) and 25°C. Initially, all the bacterial cultures were grown up to 0.4–0.5 at OD₄₅₀ in relevant media. A portion of 150 μ L from the bacterial suspensions was mixed with 50 μ L of each recombinant protein (500 ng/ μ L) in a 96-well plate. The initial OD₄₅₀ of the mixture was measured immediately using a microtiter plate reader (Multiskan EX, Thermo Scientific), and the final OD₄₅₀ was measured after 30 min of incubation at 25°C. MBP (500 ng/ μ L) and standard hen egg white lysozyme (HEWL, 500 ng/ μ L; Biosesang, Seongnam, Korea) were used as negative and positive controls, respectively. The relative antibacterial activity of each recombinant protein in terms of lytic activity against the bacterial cell wall was calculated as the difference between the initial (OD_i) and final (OD_f) absorbance. The assay was performed in triplicates to increase the reliability of the results.

Characterization of the lytic activity of recombinant AcLysC and AcLysG-like

The lytic activity of AcLysC and AcLysG-like was investigated against *M. luteus* under a range of pH and temperature conditions using a turbidimetric assay (Xue et al., 2004). *M. luteus* has commonly been used as a standard bacterial strain to study antibacterial activity and has proven to be highly susceptible to lysozyme-mediated killing (Ganz et al., 2003). Bacterial suspensions (0.8 mg/mL) of *M. luteus* (Sigma-Aldrich) were prepared in different buffers with pH ranging from 3.0 to 10.0. Buffers were prepared with sodium acetate–acetic acid (50 mM, pH 3.0–5.0), Na₂HPO₄–NaH₂PO₄ (50 mM, pH 6.0–8.0), and boric acid–NaOH (50 mM, pH 9.0–10.0). Antibacterial assays using bacterial suspensions in each buffer were conducted as described in section 2.8 with respective controls. To determine the temperature-dependence of the lytic activity of recombinant proteins, the bacterial suspension was diluted with a buffer at pH 4, and the assay was carried out at a temperature ranging from 10°C to 45°C, with intervals of 5°C. The effects of pH and temperature on the lytic activity of each recombinant protein were calculated as the difference between OD_i and OD_f absorbance values. All assays were conducted in triplicate.

Scanning electron microscope (SEM) observation

A bacterial suspension of *M. luteus* (0.8 mg/mL) was rinsed twice with phosphate buffer (pH 7.4) using two rounds of resuspension followed by centrifugation. Then, the bacterial pellet was mixed with either 500 µL of AcLysC (500 ng/µL), AcLysG-like (500 ng/µL), MBP (500 ng/µL), or molecular biology grade water. All mixtures were incubated at 25°C for 30 min and centrifuged at 16,200×g for 1 min. Each bacterial pellet was fixed in 0.1 M phosphate buffer containing 2% glutaraldehyde (pH 7.4) at room temperature for 1 h. Pellets were then dehydrated through a series of ethanol solutions (50%, 70%, 90%, 95%, and 100%) for 15 min each. Subsequently, samples were dried using liquid CO₂, followed by platinum coating using a sputter coater (Quorum Technologies, Laughton, UK). The observations were made using a MIRA3 TESCAN SEM (TESCAN, Brno, Czech Republic) at 5 kV.

Results

Sequence analysis of AcLysC and AcLysG-like

As depicted in Supplementary Fig. S1A, the ORF of *AcLysC* consisted of 429 bps, encoding for a 142 amino acid sequence with a predicted N-terminal signal peptide (Met¹-Ala¹⁷). Furthermore,

the isoelectric point (pI) and calculated molecular weight of *AcLysC* were 8.2 pI and 14.03 kDa, respectively. *AcLysC* shared the highest identity (98.6%) and similarity (98.6%) with *LysC* from *Amphiprion ocellaris*, followed by *LysC* from *P. olivaceus* (Supplementary Table S1). *AcLysG-like* contained an ORF of 570 bp encoding a protein sequence of 189 amino acids (Supplementary Fig. S1B). The pI and calculated molecular weight of *AcLysG-like* protein were 6.51 pI and 20.48 kDa, respectively. The *AcLysG-like* shared the highest identity (84.6%) and similarity (88.2%) with its homolog from *A. ocellaris* (Supplementary Table S2).

Prediction of domain organization demonstrated that both sequences contained a soluble lytic trans-glycosylase domain (SLT), catalytic residues, and sugar-binding sites (Fig. 1). According to the multiple sequence alignment, cysteine residues were mostly present in fish c-type lysozymes compared to fish g-like-type lysozymes. Furthermore, *AcLysC* shared a conserved catalytic motif with all its counterparts except for those from *Capra hircus* and *Danio rerio* (Fig. 1A). The *AcLysG-like* also contained conserved catalytic residues and sugar-binding sites, especially among fish orthologs (Fig. 1B).

To identify the molecular evolutionary relationship of *AcLysC* and *AcLysG-like* with its homologs, a phylogenetic tree was constructed using orthologs from fish, reptiles, birds, and mammals (Supplementary Fig. S2). According to the results, *AcLysC* was grouped in the clade encompassing fish c-type lysozyme and closely related to the c-type lysozyme from *A. ocellaris*. Similarly, *AcLysG-like* was clustered together with the fish g-like-type lysozymes and was closely related to its counterpart from *A. ocellaris*.

Tissue-specific expression of AcLysC and AcLysG-like, and their mRNA expression in response to immune stimulation

AcLysC and *AcLysG-like* were expressed in each selected tissue of healthy fish (Fig. 2). According to the tissue distribution of *AcLysC* (Fig. 2A), the highest expression was observed in the liver, followed by the head kidney, heart, and skin, while the lowest expression was observed in blood cells. The most prominent expression of *AcLysG-like* was observed in the heart, followed by the spleen, gill, and brain (Fig. 2B).

AcLysC and *AcLysG-like* expression after the immune stimulation with LPS, Poly I:C, and *V. harveyi* were investigated over 0–72 h p.i. in blood cells, gill, and head kidney (Figs. 3 and 4). The expression level of *AcLysC* in blood cells against each immune stimulant reached the peak (late-stage response) at 48 h p.i. In gills, the basal transcript level of *AcLysC* was remarkably upregulated

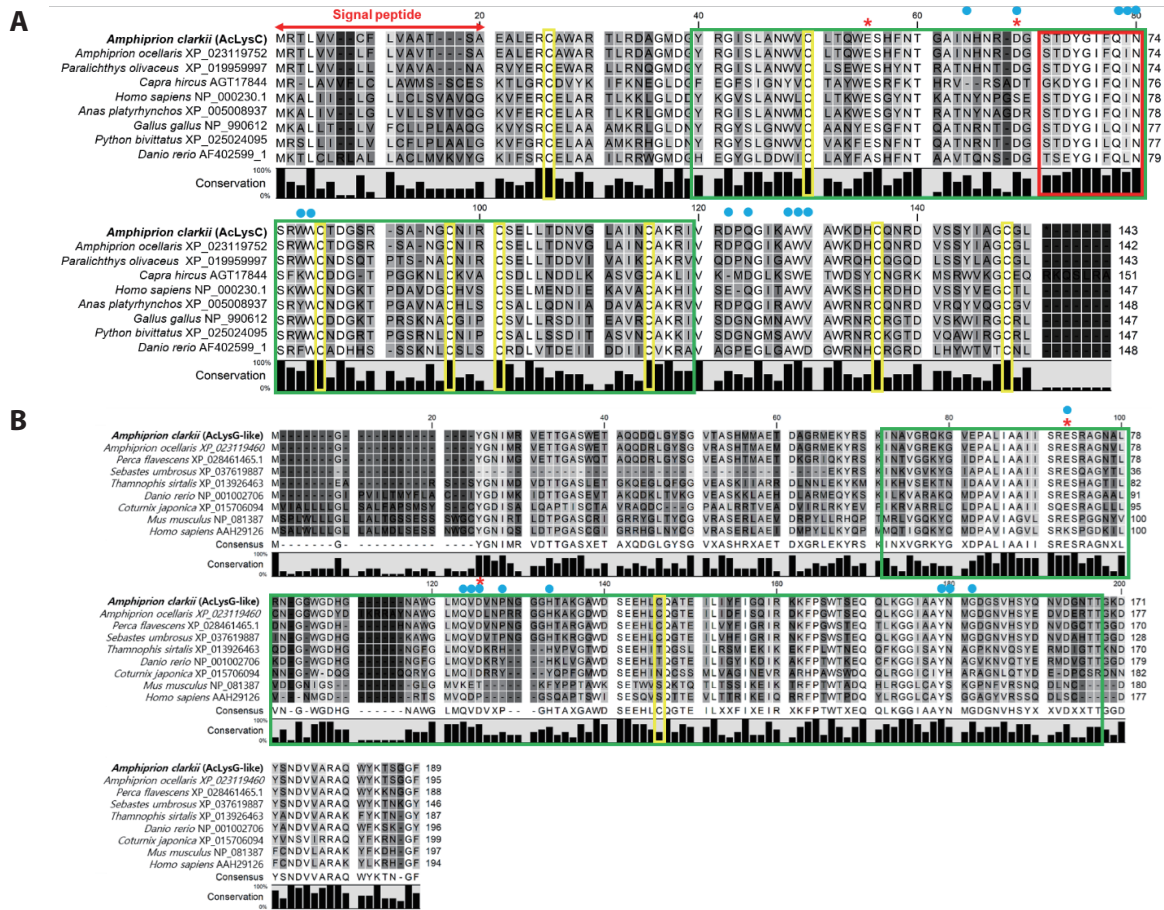


Fig. 1. Multiple sequence alignment results of (A) AcLysC (B) and AcLysG-like. Gaps are indicated by dashes. Conserved residues are represented by vertical shading ranging from white to black through ash color according to the degree of conservation of residues. The soluble lytic trans-glycosylase domain, catalytic motif, and cysteine residues are indicated by green, red, and yellow boxes, respectively. Conserved sugar-binding sites are indicated by a blue dot (●), and conserved catalytic residues are indicated by a red asterisk (*).

against all stimuli at 6 h p.i. Additionally, significant upregulation of *AcLysC* was also observed against Poly I:C and *V. harveyi* at 48 h p.i. In head kidney tissues, *AcLysC* expression was significantly ($p < 0.05$) elevated relative to its basal level in response to each immune stimulation at multiple p.i. time points. In this regard, expressional inductions against LPS and Poly I:C treatments were observed at all p.i. time points (Fig. 3C).

As depicted in Fig. 4, expressional inductions of *AcLysG-like* upon LPS and Poly I:C treatments were observed in gills and the head kidney at early phase p.i. (6 h p.i.), contrasting to what was observed for *AcLysC* in the same tissues. However, upon the experimental infection with *V. harveyi*, the expression of both *AcLysC* and *AcLysG-like* peaked at late phase p.i. (24–48 h p.i.).

Integrity and purity of AcLysC and AcLysG-like proteins

AcLysC and *AcLysG-like* were overexpressed as soluble recombinant fusion proteins with MBP by IPTG induction at 25°C for 8 h in *E. coli* ER2523. We then purified fusion proteins by affinity chromatography. The eluted recombinant fusion *AcLys* proteins (r*AcLys*) were separated and analyzed using 12% SDS-PAGE. The expected molecular weights of r*AcLysC* and r*AcLysG-like* were approximately 56.5 kDa and 62.9 kDa, respectively, as the molecular weight of MBP is approximately 42.5 kDa. Intact single bands corresponding to each expected size were observed with SDS-PAGE on their respective lanes (Supplementary Fig. S3), indicating the sufficient purity of proteins.

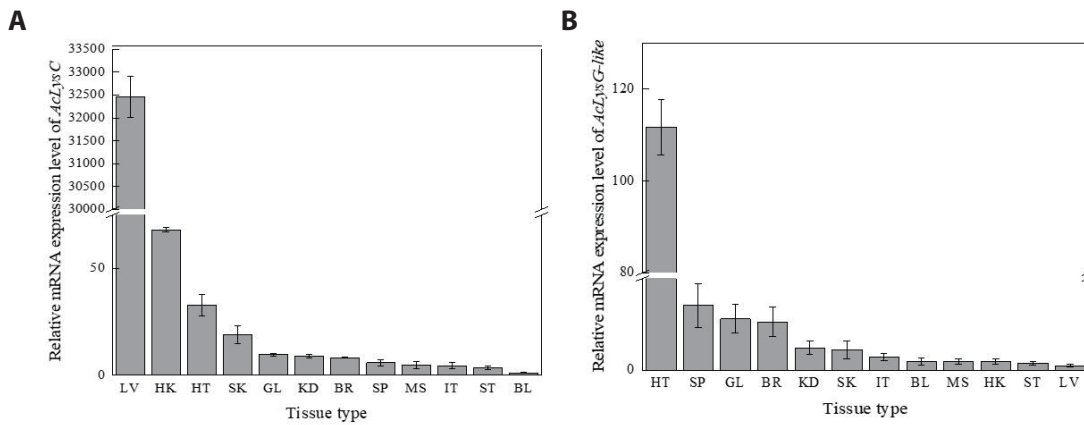


Fig. 2. Tissue-specific mRNA expression of (A) *AclLysC* and (B) *AclLysG-like*. The quantitative real-time polymerase chain reaction analysis was performed in triplicates, and the *Ef1β* gene was used as the reference gene. Data were represented as mean ± SD. HT: heart; SP: spleen; GL: gill; BR: brain; KD: kidney; IT: intestine; BL: blood; MS: muscle; HK: head kidney; ST: stomach; LV: liver; SK: skin.

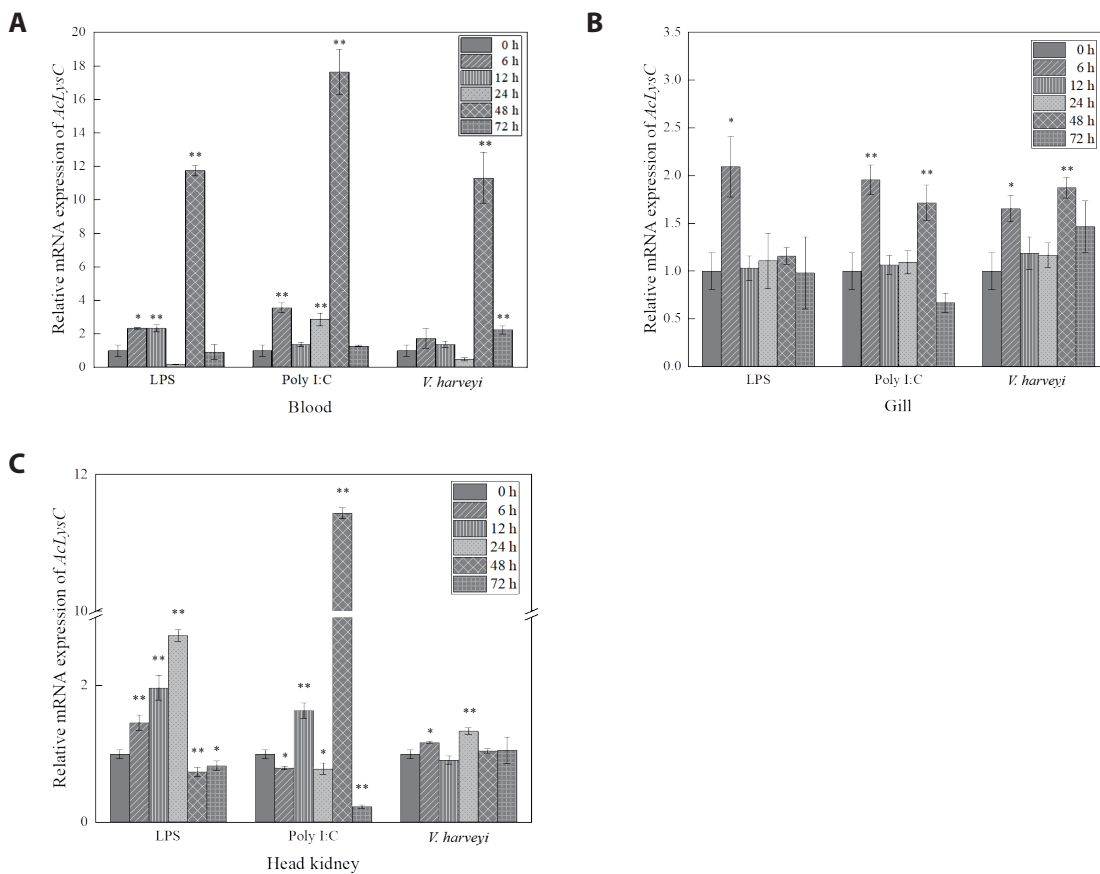


Fig. 3. Relative mRNA expression of *AclLysC* in the (A) blood, (B) gill, and (C) head kidney against different immune stimulants. mRNA levels of *AclLysC* were calculated using the $2^{-\Delta\Delta CT}$ method, and *Ef1β* was used as the reference gene. The relative fold changes were normalized relative to those of the phosphate-buffered saline-injected control at different time points. The results are reported as mean ± SD of experimental triplicates. Statistical differences compared to the 0 h post-injection are indicated by asterisks; * $p < 0.05$ and ** $p < 0.01$. LPS, lipopolysaccharide; Poly I:C, polyinosinic: polycytidylic acid.

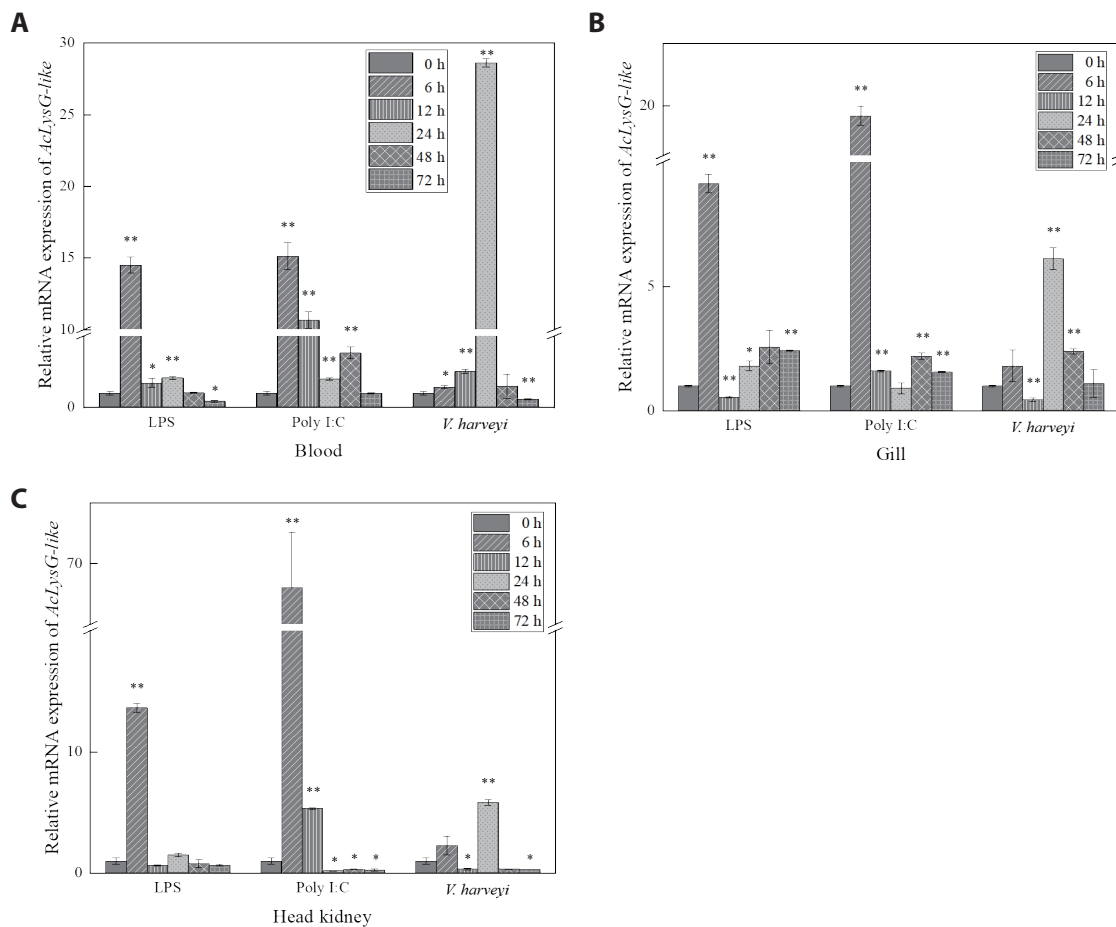


Fig. 4. Relative mRNA expression of AcLysG-like in (A) blood, (B) gill, and (C) head kidney against different immune stimulants. mRNA levels of AcLysG-like were calculated using the $2^{-\Delta\Delta CT}$ method, and *Ef1 β* was used as the reference gene. The relative fold changes were normalized with those of the phosphate-buffered saline-injected control at different time points. The results are reported as mean \pm SD of experimental triplicates. Statistical differences compared to the 0 h post-injection are indicated by asterisks; * $p < 0.05$ and ** $p < 0.01$. LPS, lipopolysaccharide; Poly I:C, polyinosinic: polycytidylic acid.

Functional study of AcLysC and AcLysG-like

Antibacterial activity of AcLysC and AcLysG-like against fish pathogens

As shown in Fig. 5, the antibacterial activities of AcLysC and AcLysG-like were observed against different marine bacterial pathogens. Particularly, AcLysG-like had more pronounced antibacterial activity against most bacteria compared to that of AcLysC and HEWL. AcLysC exhibited lower antibacterial activity against most bacteria used in the study compared to the positive control HEWL. However, AcLysC showed its highest antibacterial activity against *V. anguillarum*, and HEWL showed more prominent antibacterial activity against *M. luteus*.

Effect of pH and temperature on antibacterial activity of AcLysC and AcLysG-like

To investigate the modulation of antibacterial activity of AcLysC and AcLysG-like with pH and temperature, the bactericidal activity of recombinant fusion proteins was assessed under a range of pH and temperatures against *M. luteus*, with MBP and HEWL as controls. Results showed that both AcLysC and AcLysG-like exhibit their highest bacteriolytic enzymatic activity at pH 4.0. The highest enzymatic activity of HEWL (positive control) was observed at pH 8 (Fig. 6A). Additionally, AcLysC was found to be noticeably active at moderately high temperatures (35 °C–40 °C), while AcLysG-like was active at lower temperatures (10 °C–15 °C) (Fig. 6B). HEWL showed the highest activity at 30 °C, whereas no significant

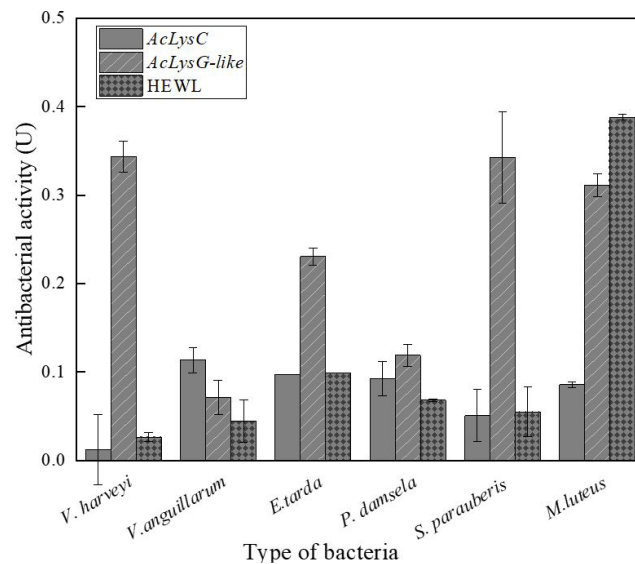


Fig. 5. Antibacterial activity assay of AcLysC and AcLysG-like against gram-negative bacteria (*Vibrio harveyi*, *Vibrio anguillarum*, *Edwardsiella tarda*, *Photobacterium damsela* subsp. *piscicida*) and gram-positive bacteria (*Streptococcus parauberis* and *Micrococcus luteus*). HEWL was used as the positive control. HEWL, hen egg white lysozyme.

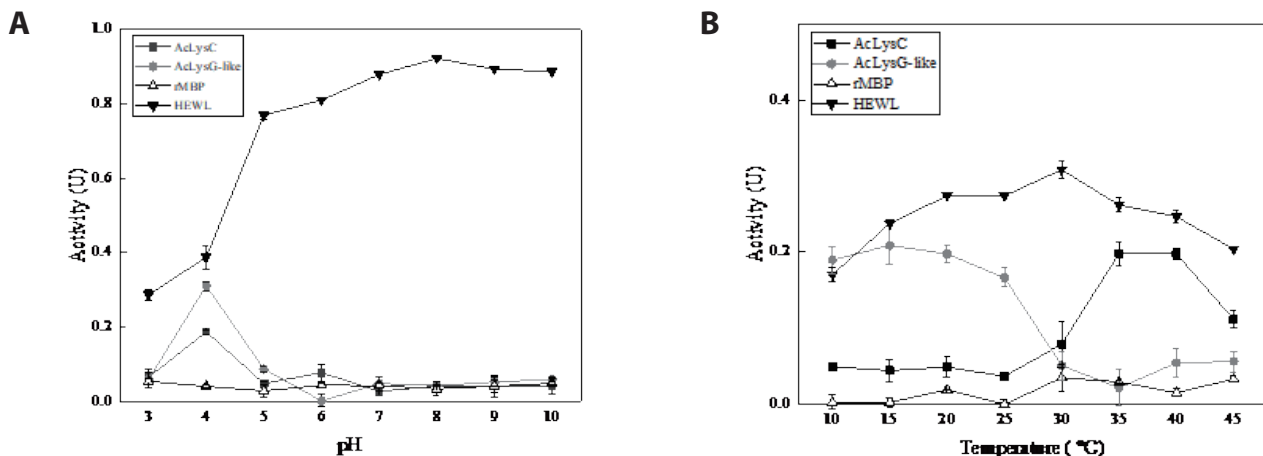


Fig. 6. Effect of (A) pH and (B) temperature on *Micrococcus luteus* bactericidal activity of recombinant AcLysC and AcLysG-like. MBP, maltose-binding protein; HEWL, hen egg white lysozyme.

activity was detected for MBP under tested pH and temperature conditions.

Scanning electron microscope (SEM) observation

To observe the morphological changes that occurred due to the bacteria lytic activities of the two proteins, the cell surface of *M. luteus* was filmed using a scanning electron microscope (SEM;

MIRA3 TESCAN). Generally, naïve *M. luteus* cells have a smooth surface with a spherical (coccus) shape. Expectedly, both the H₂O- and MBP-treated samples showed clear and smooth cell surfaces (Fig. 7A and 7B). In contrast, *M. luteus* treated with HEWL (Fig. 7C), AcLysC (Fig. 7D), and AcLysG-like (Fig. 7E) showed wrinkled, shrunken, and fractured cell walls, evidencing cell lysis.

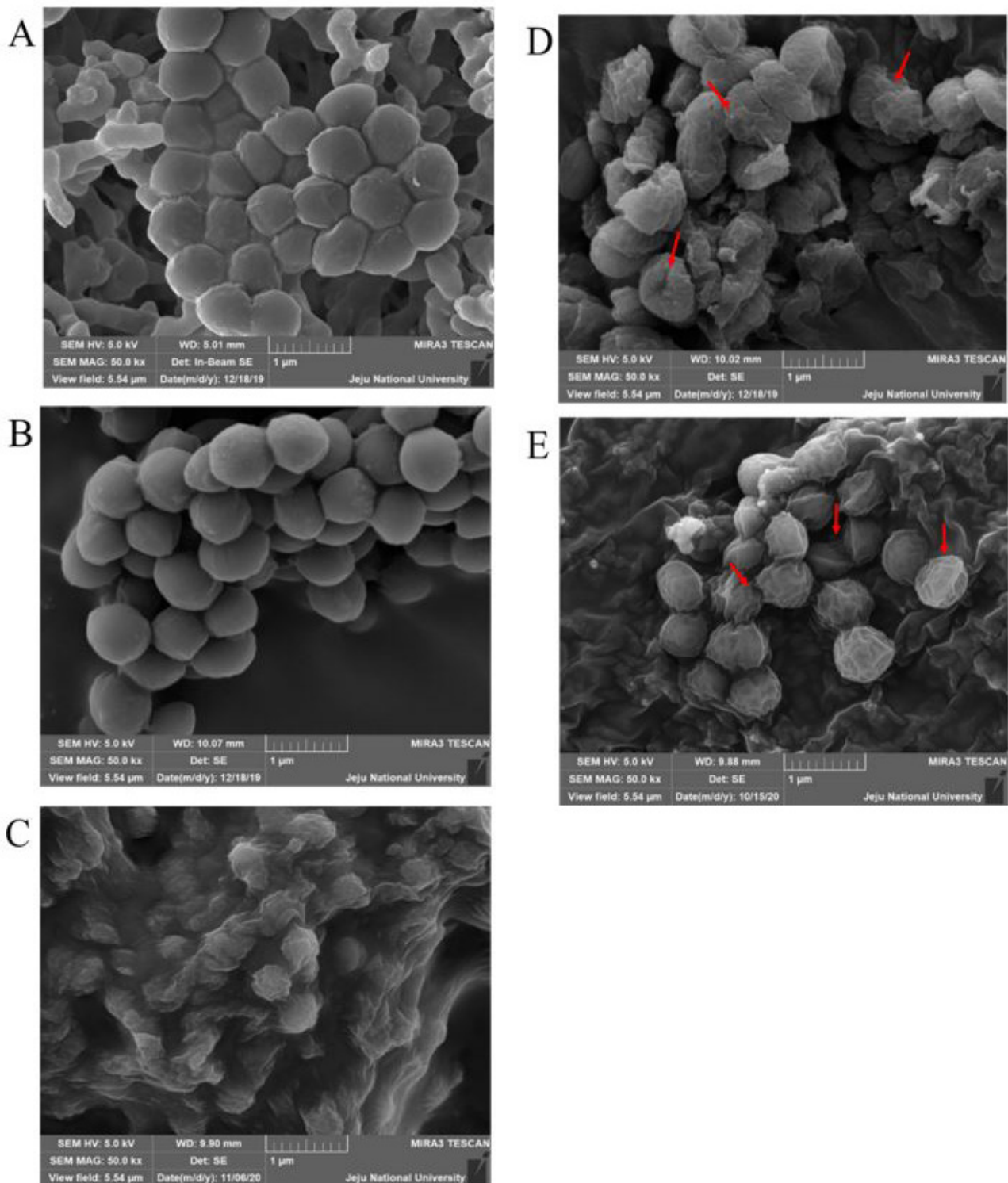


Fig. 7. The morphological changes of *Micrococcus luteus* observed under a scanning electron microscope (MIRa3 TESCAN, at 5 kV) after being treated with (A) triple-distilled water, (B) maltose-binding protein, (C) hen egg white lysozyme, (D) AclysC, and (E) AclysG-like.

Discussion

Lysozyme is one of the most important antibacterial proteins involved in host innate immune mechanisms of the host. It breaks the peptidoglycan layer of the cell wall, thus promoting the lysis of bacterial cells (Jollès & Jollès, 1984). Furthermore, lysozyme can be found in many organisms, including bacteriophages, microbes, plants, invertebrates, and vertebrates. It shows antibacterial activity against various bacteria and controls the release of pathogen-associated molecular patterns (PAMPs), hormones, and (Whang et al., 2011; Zhao et al., 2011) involved in the regulation of immune responses (Ragland & Criss, 2017).

According to the *in silico* analysis, both AcLyC and AcLyG-like contain the SLT domain, which plays a critical role in the hydrolysis of β -1,4-glycosidic bonds between N-acetylmuramic acid and N-acetylglucosamine of the peptidoglycan layer in the cell wall (Whang et al., 2011). In addition, *AcLysC* harbors a conserved sugar-binding site, cysteine residues, and catalytic residues in common with those found in other species. The *AcLysC* protein sequence comprises a high content of well-conserved cysteine residues, which are known to form four intra-disulfide bonds that might provide high stability and osmolarity against seawater and proteases (Ito et al., 1999). These disulfide bridges are considered to remarkably affect the catalytic function, secretion processes, and structural stabilization by maintaining the molecular integrity and elliptical shape of the protein (Kato et al., 1981). Additionally, a signal peptide sequence in *AcLysC* can help secrete the protein extracellularly, as observed for most known c-type lysozymes (Cai et al., 2019). Extracellular lysozymes also break down the peptidoglycan layer into soluble fragments, enabling PAMP recognition by nucleotide-binding oligomerization domain-containing protein receptors in mucous epithelial cells, which stimulate the chemical maintenance and secretion of immune activation factors in macrophages (Ragland & Criss, 2017). On the other hand, the *AcLysG-like* protein sequence lacks disulfide bonds (only one cysteine residue) and a signal peptide. Therefore, *AcLysG-like* can be considered an intracellular protein. Moreover, previous reports on fish such as Atlantic cod (*Gadus morhua* L.) (Larsen et al., 2009), olive flounder (*P. olivaceus*) (Hikima et al., 2001), and orange-spotted grouper (*E. coioides*) (Wei et al., 2012) confirmed the absence of cysteines in g-type lysozymes. However, the number of cysteine residues in g-type lysozymes varies depending on the species (Kawamura et al., 2006; Kawamura et al., 2008).

According to a previous study, the lysozyme content of fish

organs can differ based on the species (Subbotkina & Subbotkin, 2003). Furthermore, lysozyme showed higher expression in the kidney, spleen, and liver compared to other tissues of many fish species (Gao et al., 2012; Jiménez-Cantizano et al., 2008; Wang et al., 2016). According to the tissue-specific expression patterns observed in this study, the highest *AcLysC* mRNA expression level was detected in the liver, the main organ involved in metabolism, detoxification, and hematopoiesis in fish (Rui, 2014). Lysozymes play an additional role in nutrient absorption in animals (Callewaert & Michiels, 2010). For instance, rabbits have unique behavior, “coprophagia,” a nutritional strategy to absorb large amounts of lysozyme from soft feces (Cámara & Prieur, 1984). Fish can be continuously exposed to various pathogens during feeding. Thus, the liver and its secretions, such as the bile, could contain a high amount of lysozyme as a defensive mechanism. Furthermore, fish c-type lysozymes showed high mRNA levels depending on various factors, such as stress, intensity, and diseases (Caruso et al., 2002). Therefore, it is likely to observe pronounced expression of *AcLysC* in liver tissues.

In contrast, g-type lysozymes are specialized to play a distinct role in antibacterial activity (Saurabh & Sahoo, 2008). The highest expression level of *AcLysG-like* was observed in the heart, followed by that in the spleen and gills. A similar mRNA expression pattern was earlier detected in olive flounder (*P. olivaceus*) (Hikima et al., 2001). The heart and spleen are reportedly involved in the clearance of blood-borne substances, particularly in some fish species like *G. morhua*, and endothelial cells of the heart were found to be involved in the endocytosis of circulating substances. In contrast, gills can act as a barrier to the entry of pathogens and are enriched with leucocytes which can contribute to the local immune responses (Press & Evensen, 1999). Thus, intracellular lysozymes such as *AcLysG-like* seemingly exert bacteriolytic functions to protect the host from infections.

Based on the temporal mRNA expression, the defensive roles of *AcLysC* and *AcLysG-like* against LPS, Poly I:C, and *V. harveyi* were investigated in blood cells, gill, and head kidney tissues. Unlike those of mammals, fish red blood cells are nucleated and can trigger immune responses against immune stimulants (Morera & MacKenzie, 2011). However, peripheral white blood cells, such as macrophages and neutrophils, which act as first-line barriers to pathogenic infections, abundantly express lysozymes. Macrophages and neutrophils engulf pathogens and kill them via lysozyme-mediated degradation (Callewaert & Michiels, 2010). Therefore, lysozymes in fish blood cells may play a vital role in combating infections. Fish gills are more susceptible to infectious pathogens

due to their continuous exposure to ambient water that circulates during respiration. The fish head kidney is analogous to the adrenal gland of mammals and is a leukocyte-rich immune organ that subsequently activates several other immune mechanisms in other tissues (Geven & Klaren, 2017; Paulsen et al., 2003). Expectedly, the expression of AcLysC and AcLysG-like was significantly modulated by immune stimulants in these tissues.

An endotoxic immune modulator, LPS, is known to induce lysozyme production through Toll-like family receptors or cytokines (Jiménez-Cantizano et al., 2008). LPS stimulation induced lysozyme upregulation in brill (*Scophthalmus rhombus*) (Yildiz, 2006) and yellow catfish (*Pelteobagrus fulvidraco*) (Liu et al., 2016). Similarly, significant upregulation of AcLysC and AcLysG-like mRNA levels was observed in the blood, gill, and head kidney tissues after LPS treatment.

Poly I:C is a synthetic compound that, like a double-stranded RNA virus, stimulates an antiviral immune response. Previous studies have provided evidence for the antiviral activity of lysozyme (Lee-Huang et al., 1999; Mai & Wang, 2010; Takahashi et al., 2018; Zhang et al., 2008). Lysozymes in chicken egg white, human milk, and human neutrophils have been shown to degrade the viral RNA of human immunodeficiency virus (Lee-Huang et al., 1999). Given this background, the observed inductive expressional responses of AcLysC and AcLysG-like upon Poly I:C treatment suggest their potential role in antibacterial and antiviral defense in the piscine innate immune system.

V. harveyi is a gram-negative marine bacterium that is associated with a broad spectrum of diseases in fish (Zhang et al., 2020). Although gram-negative bacteria are less vulnerable to lysozymes, basal expression of both AcLysC and AcLysG-like were upregulated after *V. harveyi* challenge. However, AcLysG-like induced its basal expression with a higher fold than that of AcLysC post-experimental infection with *V. harveyi*. A similar pattern was observed in grass carp when challenged with *Aeromonas hydrophila* (Ye et al., 2010). Therefore, AcLysG-like might be more sensitive against *V. harveyi* than AcLysC in host immune defense. In contrast to the AcLysG-like responses against LPS and Poly I:C, upregulation was detected at a later phase against *V. harveyi* infection. This observation can be attributed to the fact that the piscine innate immune system requires more time to respond to the live pathogens compared to PAMPs such as LPS and Poly I:C. Live pathogens may have additional patterns deriving from the strategies that are used to invade, manipulate, replicate within, or spread among their hosts (Vance et al., 2009).

Several studies on animals such as barramundi (*Lates*

calcarifer) (Fu et al., 2013), silkworm (*Bombyx mori*) (Chen et al., 2018), Farrer's scallop (*Chlamys farreri*) (Zhao et al., 2007), grass carp (*Ctenopharyngodon idellus*) (Ye et al., 2010), and Chinese perch (*Siniperca chuatsi*) (Sun et al., 2006) have shown that recombinant lysozymes exert promising antimicrobial activity against bacterial pathogens. The selected bacterial species in this study such as *E. tarda*, *P. damsela* subsp. *piscicida*, *V. anguillarum*, *V. harveyi*, and *S. parauberis* are well-known disease-causing pathogens of mariculture fish (Austin & Zhang, 2006; Blazer, 1988; Currás et al., 2002; Rivas et al., 2013). According to our results, AcLysG-like demonstrated more pronounced antibacterial activity against most bacterial pathogens used in the study. Further, it showed profound activity against both gram-negative and gram-positive bacteria compared to AcLysC. Lysozymes are known to show stronger bacteriolytic activity against gram-positive than gram-negative bacteria (Saurabh & Sahoo, 2008; Silveti et al., 2017) but they can also extend activity against gram-negative bacteria through denaturation, chemical modifications, or by combining themselves with other preservatives (Silveti et al., 2017). Apart from that, it is reported that g-type lysozymes are able to bind to both gram-positive and negative bacterial cell wall components (LPS (Lipopolysaccharide), PGN (Peptidoglycan), and LTA (Lipoteichoic acid)) without significant differences (Liu et al., 2022). Moreover, it is speculated that g-like type lysozymes are able to cause more denaturation or chemical modifications in bacteria than c-type lysozyme, which contains numerous cysteine residues with stable disulfide bonds (Clarke et al., 2000; Kawamura et al., 2008). AcLysC showed relatively low antibacterial activity against *V. harveyi*. One possible explanation behind this observation is the antibacterial resistance of this bacterium to lysozyme either by altering the cell wall structure or through covalent binding with other polymers of the peptidoglycan cell wall (Bera et al., 2006; Callewaert et al., 2012; Raymond et al., 2005). Additionally, we observed that AcLysG-like showed different antimicrobial activity against *V. anguillarum* and *V. harveyi*. Several reports suggest that g-type lysozymes show different rates of antimicrobial activity with bacterial species from the same genus such as *V. tapetis* and *V. anguillarum* (Nilojan et al., 2017), and *S. aureus* and *S. iniae* (Wei et al., 2014). The reason might be that g-type lysozyme has a different binding ability to bacteria or bacteria cell wall components. Due to these different binding abilities, g-type lysozymes selectively kill gram-negative bacteria in a non-enzymatic mode by damaging bacterial membranes (Luo et al., 2021). Collectively both lysozymes can be proposed as potential players in the host antibacterial defense in *A. clarkii*. The differential activities of two AcLys against the same pathogen may

reflect the pathogenetic differences underlying bacterial diseases or the consequences of distinct infection routes (Wang et al., 2013). Previous studies have suggested that g-type lysozyme may be induced for defense against invading pathogens, whereas c-type lysozyme might be the major molecule for housekeeping defense under normal conditions (Ye et al., 2010). This notion can also be inferred by comparing the antibacterial activities observed for rAcLysG-like with rAcLysC in this study.

Recombinant AcLysC was noticeably active at lower pH (pH 4) and moderately high temperatures (35 °C–40 °C). Similar observations have been reported for disk abalone (*Haliotis discus discus*) (Umasuthan et al., 2013) and Mediterranean mussel (*Mytilus galloprovincialis*) (Wang et al., 2013), showing that their c-type lysozymes have pronounced activity at low pH. Like AcLysC, AcLysG-like also showed its optimum activity at low pH (pH 4). Previously, g-type lysozymes were reported to be active at low pH in black rockfish (*Sebastes schlegelii*) (Nilojan et al., 2017), big-belly seahorse (*H. abdominalis*) (Ko et al., 2016), rock bream (*Oplegnathus fasciatus*) (Whang et al., 2011), and disk abalone (*H. discus discus*) (Bathige et al., 2013).

The optimum temperature of enzymes was shown to depend on the number of disulfide bonds (Li et al., 1998; Yin et al., 2015). The AcLysC sequence contains eight cysteine residues. However, AcLysG-like contains only one cysteine residue. According to our observation, rAcLysC, which can potentially form more disulfide bonds, likely demonstrate its optimal activity at a higher temperature range compared to rAcLysG-like.

Scanning electron microscope examination of *M. luteus* following rAcLys treatments evidenced morphological changes in the bacterial cell wall. The surface changes of *M. luteus* observed after the treatments reinforced the detected antibacterial activities of rAcLys using the turbidimetric assay.

Conclusion

In summary, AcLysC and AcLysG-like lysozyme sequences of *A. clarkii* were conserved relative to those of other homologs and were closely related to *A. ocellaris* orthologs. The highest tissue-specific mRNA levels of AcLysC and AcLysG-like were observed in the liver and the heart, respectively. Furthermore, AcLysC and AcLysG-like were upregulated in the gill, head kidney, and blood cells following immune stimulation. Recombinant AcLysC and AcLysG-like proteins showed antibacterial activity against all tested fish pathogens with the highest lytic activity at pH 4. The SEM observations provided conclusive evidence of the lytic activity of

AcLysC and AcLysG-like on the cell wall of *M. luteus*. Altogether, the findings of this study suggest that AcLysC and AcLysG-like play a crucial role in the innate immune system of *A. clarkii* by defending against invading microbial pathogens.

Supplementary Materials

Supplementary materials are only available online from: <https://doi.org/10.47853/FAS.2023.e16>

Competing interests

No potential conflict of interest relevant to this article was reported.

Funding sources

This research was supported by the Korea Institute of Marine Science & Technology Promotion (KIMST), funded by the Ministry of Oceans and Fisheries (20220570).

Acknowledgements

Not applicable.

Availability of data and materials

Upon reasonable request, the datasets of this study can be available from the corresponding author.

Ethics approval and consent to participate

All experimental procedures involved in this study were reviewed and approved by the Animal Care and Use Committee of the Jeju National University (approval no. 2022-0042).

ORCID

Gaeun Kim	https://orcid.org/0000-0002-1733-052X
Hanchang Sohn	https://orcid.org/0000-0002-9811-4609
WKM Omeka	https://orcid.org/0000-0002-1004-1645
Chaehyeon Lim	https://orcid.org/0000-0002-9977-561X
Don Anushka Sandaruwan Elvitigala	https://orcid.org/0000-0002-3175-1531
Jehee Lee	https://orcid.org/0000-0001-9144-3648

References

- Austin B, Zhang XH. *Vibrio harveyi*: a significant pathogen of marine vertebrates and invertebrates. *Lett Appl Microbiol*. 2006;43:119-24.
- Avella MA, Olivotto I, Gioacchini G, Maradonna F, Carnevali

- O. The role of fatty acids enrichments in the larviculture of false percula clownfish *Amphiprion ocellaris*. *Aquaculture*. 2007;273:87-95.
- Bathige SDNK, Umasuthan N, Whang I, Lim BS, Jung HB, Lee J. Evidences for the involvement of an invertebrate goose-type lysozyme in disk abalone immunity: cloning, expression analysis and antimicrobial activity. *Fish Shellfish Immunol*. 2013;35:1369-79.
- Bera A, Biswas R, Herbert S, Götz F. The presence of peptidoglycan O-acetyltransferase in various staphylococcal species correlates with lysozyme resistance and pathogenicity. *Infect Immun*. 2006;74:4598-604.
- Blazer VS. Bacterial fish pathogens. *Environ Biol Fishes*. 1988;21:77-9.
- Cai S, Zhang Y, Wu F, Wu R, Yang S, Li Y, et al. Identification and functional characterization of a c-type lysozyme from *Fenneropenaeus penicillatus*. *Fish Shellfish Immunol*. 2019;88:161-9.
- Callewaert L, Michiels CW. Lysozymes in the animal kingdom. *J Biosci*. 2010;35:127-60.
- Callewaert L, Van Herreweghe JM, Vanderkelen L, Leysen S, Voet A, Michiels CW. Guards of the great wall: bacterial lysozyme inhibitors. *Trends Microbiol*. 2012;20:501-10.
- Cámara VM, Prieur DJ. Secretion of colonic isozyme of lysozyme in association with cecotrophy of rabbits. *Am J Physiol Gastrointest Liver Physiol*. 1984;247:G19-23.
- Caruso D, Schlumberger O, Dahm C, Proteau JP. Plasma lysozyme levels in sheatfish *Silurus glanis* (L.) subjected to stress and experimental infection with *Edwardsiella tarda*. *Aquac Res*. 2002;33:999-1008.
- Chen T, Tan L, Hu N, Dong Z, Hu Z, Jiang Y, et al. C-lysozyme contributes to antiviral immunity in *Bombyx mori* against nucleopolyhedrovirus infection. *J Insect Physiol*. 2018;108:54-60.
- Clarke J, Hounslow AM, Bond CJ, Fersht AR, Daggett V. The effects of disulfide bonds on the denatured state of barnase. *Protein Sci*. 2000;9:2394-404.
- Currás M, Magariños B, Toranzo AE, Romalde JL. Dormancy as a survival strategy of the fish pathogen *Streptococcus parauberis* in the marine environment. *Dis Aquat Organ*. 2002;52:129-36.
- Fu GH, Bai ZY, Xia JH, Liu F, Liu P, Yue GH. Analysis of two lysozyme genes and antimicrobial functions of their recombinant proteins in Asian seabass. *PLOS ONE*. 2013;8:e79743.
- Ganz T, Gabayan V, Liao HI, Liu L, Oren A, Graf T, et al. Increased inflammation in lysozyme M-deficient mice in response to *Micrococcus luteus* and its peptidoglycan. *Blood*. 2003;101:2388-92.
- Gao F, Qu L, Yu S, Ye X, Tian Y, Zhang L, et al. Identification and expression analysis of three c-type lysozymes in *Oreochromis aureus*. *Fish Shellfish Immunol*. 2012;32:779-88.
- Geven EJW, Klaren PHM. The teleost head kidney: integrating thyroid and immune signalling. *Dev Comp Immunol*. 2017;66:73-83.
- Hancock REW, Scott MG. The role of antimicrobial peptides in animal defenses. *Proc Natl Acad Sci USA*. 2000;97:8856-61.
- Harikrishnan R, Kim JS, Kim MC, Balasundaram C, Heo MS. Molecular characterization, phylogeny, and expression pattern of c-type lysozyme in kelp grouper, *Epinephelus bruneus*. *Fish Shellfish Immunol*. 2011;31:588-94.
- Hikima J, Minagawa S, Hirono I, Aoki T. Molecular cloning, expression and evolution of the Japanese flounder goose-type lysozyme gene, and the lytic activity of its recombinant protein. *Biochim Biophys Acta Gene Struct Expr*. 2001;1520:35-44.
- Ito Y, Yoshikawa A, Hotani T, Fukuda S, Sugimura K, Imoto T. Amino acid sequences of lysozymes newly purified from invertebrates imply wide distribution of a novel class in the lysozyme family. *Eur J Biochem*. 1999;259:456-61.
- Jiménez-Cantizano RM, Infante C, Martín-Antonio B, Ponce M, Hachero I, Navas JI, et al. Molecular characterization, phylogeny, and expression of c-type and g-type lysozymes in brill (*Scophthalmus rhombus*). *Fish Shellfish Immunol*. 2008;25:57-65.
- Jollès P, Jollès J. What's new in lysozyme research?: always a model system, today as yesterday. *Mol Cell Biochem*. 1984;63:165-89.
- Kato S, Okamura M, Shimamoto N, Utiyama H. Spectral evidence for a rapidly formed structural intermediate in the refolding kinetics of hen egg-white lysozyme. *Biochemistry*. 1981;20:1080-5.
- Kawamura S, Ohkuma M, Chijiwa Y, Kohno D, Nakagawa H, Hirakawa H, et al. Role of disulfide bonds in goose-type lysozyme. *FEBS J*. 2008;275:2818-30.
- Kawamura S, Ohno K, Ohkuma M, Chijiwa Y, Torikata T. Experimental verification of the crucial roles of Glu⁷³ in the catalytic activity and structural stability of goose type lysozyme. *J Biochem*. 2006;140:75-85.
- Ko J, Wan Q, Bathige SDNK, Lee J. Molecular characterization, transcriptional profiling, and antibacterial potential of G-type lysozyme from seahorse (*Hippocampus abdominalis*). *Fish Shellfish Immunol*. 2016;58:622-30.
- Kokoshis PL, Williams DL, Cook JA, Di Luzio NR. Increased resistance to *Staphylococcus aureus* infection and enhancement in serum lysozyme activity by glucan. *Science*. 1978;199:1340-2.
- Larsen AN, Solstad T, Svineng G, Seppola M, Jørgensen TØ. Molecular characterisation of a goose-type lysozyme gene in Atlantic

- cod (*Gadus morhua* L.). *Fish Shellfish Immunol.* 2009;26:122-32.
- Lee-Huang S, Huang PL, Sun Y, Huang PL, Kung H, Blithe DL, et al. Lysozyme and RNases as anti-HIV components in β -core preparations of human chorionic gonadotropin. *Proc Natl Acad Sci USA.* 1999;96:2678-81.
- Li C, Zhao Y, Liu T, Huang J, Zhang Q, Liu B, et al. The distribution and function characterization of the i type lysozyme from *Apostichopus japonicus*. *Fish Shellfish Immunol.* 2018;74:419-25.
- Li H, Wei X, Yang J, Zhang R, Zhang Q, Yang J. The bacteriolytic mechanism of an invertebrate-type lysozyme from mollusk *Octopus ocellatus*. *Fish Shellfish Immunol.* 2019;93:232-9.
- Li Y, Coutinho PM, Ford C. Effect on thermostability and catalytic activity of introducing disulfide bonds into *Aspergillus awamori* glucoamylase. *Protein Eng Des Sel.* 1998;11:661-7.
- Liu QN, Xin ZZ, Zhang DZ, Jiang SH, Chai XY, Li CF, et al. Molecular identification and expression analysis of a goose-type lysozyme (LysG) gene in yellow catfish *Pelteobagrus fulvidraco*. *Fish Shellfish Immunol.* 2016;58:423-8.
- Liu Y, Zha H, Yu S, Zhong J, Liu X, Yang H, et al. Molecular characterization and antibacterial activities of a goose-type lysozyme gene from roughskin sculpin (*Trachidermus fasciatus*). *Fish Shellfish Immunol.* 2022;127:1079-87.
- Livak KJ, Schmittgen TD. Analysis of relative gene expression data using real-time quantitative PCR and the $2^{-\Delta\Delta CT}$ method. *Methods.* 2001;25:402-8.
- Luo JC, Zhang J, Sun L. A g-type lysozyme from deep-sea hydrothermal vent shrimp kills selectively gram-negative bacteria. *Molecules.* 2021;26:7624.
- Mai W, Wang W. Protection of blue shrimp (*Litopenaeus stylirostris*) against the white spot syndrome virus (WSSV) when injected with shrimp lysozyme. *Fish Shellfish Immunol.* 2010;28:727-33.
- Morera D, MacKenzie SA. Is there a direct role for erythrocytes in the immune response? *Vet Res.* 2011;42:89.
- Nilojan J, Bathige SDNK, Kugapreethan R, Thulasitha WS, Nam BH, Lee J. Molecular, transcriptional and functional insights into duplicated goose-type lysozymes from *Sebastes schlegelii* and their potential immunological role. *Fish Shellfish Immunol.* 2017;67:66-77.
- Paulsen SM, Lunde H, Engstad RE, Robertsen B. *In vivo* effects of β -glucan and LPS on regulation of lysozyme activity and mRNA expression in Atlantic salmon (*Salmo salar* L.). *Fish Shellfish Immunol.* 2003;14:39-54.
- Press CML, Evensen Ø. The morphology of the immune system in teleost fishes. *Fish Shellfish Immunol.* 1999;9:309-18.
- Pridgeon JW, Klesius PH, Dominowski PJ, Yancey RJ, Kievit MS. Chicken-type lysozyme in channel catfish: expression analysis, lysozyme activity, and efficacy as immunostimulant against *Aeromonas hydrophila* infection. *Fish Shellfish Immunol.* 2013;35:680-8.
- Prilusky J, Hodis E, Canner D, Decatur WA, Oberholser K, Martz E, et al. Proteopedia: a status report on the collaborative, 3D web-encyclopedia of proteins and other biomolecules. *J Struct Biol.* 2011;175:244-52.
- Ragland SA, Criss AK. From bacterial killing to immune modulation: recent insights into the functions of lysozyme. *PLOS Pathog.* 2017;13:e1006512.
- Raymond JB, Mahapatra S, Crick DC, Pavelka MS Jr. Identification of the *namH* gene, encoding the hydroxylase responsible for the N-glycolylation of the mycobacterial peptidoglycan. *J Biol Chem.* 2005;280:326-33.
- Rivas AJ, Lemos ML, Osorio CR. *Photobacterium damsela* subsp. *damsela*, a bacterium pathogenic for marine animals and humans. *Front Microbiol.* 2013;4:283.
- Roux N, Salis P, Lee SH, Besseau L, Laudet V. Anemonefish, a model for Eco-Evo-Devo. *Evodevo.* 2020;11:20.
- Rui L. Energy metabolism in the liver. *Compr Physiol.* 2014;4:177-97.
- Saurabh S, Sahoo PK. Lysozyme: an important defence molecule of fish innate immune system. *Aquac Res.* 2008;39:223-39.
- Sava G, Ceschia V, Zabucchi G. Evidence for host-mediated antitumor effects of lysozyme in mice bearing the MCa mammary carcinoma. *Eur J Cancer Clin Oncol.* 1988;24:1737-43.
- Silvetti T, Morandi S, Hintersteiner M, Brasca M. Use of hen egg white lysozyme in the food industry. In: Hester PY, editor. *Egg innovations and strategies for improvements.* London: Elsevier; 2017. p. 233-42.
- Smith KF, Schmidt V, Rosen GE, Amaral-Zettler L. Microbial diversity and potential pathogens in ornamental fish aquarium water. *PLOS ONE.* 2012;7:e39971.
- Subbotkina TA, Subbotkin MF. Lysozyme content in organs and blood serum in various species in the volga river. *J Evol Biochem Physiol.* 2003;39:537-46.
- Sun BJ, Wang GL, Xie HX, Gao Q, Nie P. Gene structure of goose-type lysozyme in the mandarin fish *Siniperca chuatsi* with analysis on the lytic activity of its recombinant in *Escherichia coli*. *Aquaculture.* 2006;252:106-13.
- Takahashi M, Okakura Y, Takahashi H, Imamura M, Takeuchi A,

- Shidara H, et al. Heat-denatured lysozyme could be a novel disinfectant for reducing hepatitis A virus and murine norovirus on berry fruit. *Int J Food Microbiol.* 2018;266:104-8.
- Umasuthan N, Bathige SDNK, Kasthuri SR, Wan Q, Whang I, Lee J. Two duplicated chicken-type lysozyme genes in disc abalone *Haliotis discus discus*: molecular aspects in relevance to structure, genomic organization, mRNA expression and bacteriolytic function. *Fish Shellfish Immunol.* 2013;35:284-99.
- Vance RE, Isberg RR, Portnoy DA. Patterns of pathogenesis: discrimination of pathogenic and nonpathogenic microbes by the innate immune system. *Cell Host Microbe.* 2009;6:10-21.
- Wang M, Zhao X, Kong X, Wang L, Jiao D, Zhang H. Molecular characterization and expressing analysis of the c-type and g-type lysozymes in Qihe crucian carp *Carassius auratus*. *Fish Shellfish Immunol.* 2016;52:210-20.
- Wang Q, Wang C, Mu C, Wu H, Zhang L, Zhao J. A novel C-type lysozyme from *Mytilus galloprovincialis*: insight into innate immunity and molecular evolution of invertebrate c-type lysozymes. *PLOS ONE.* 2013;8:e67469.
- Wei Q, Mu C, Wang C, Zhao J. Molecular characterization, expression, and antibacterial activity of a c-type lysozyme isolated from the manila clam, *Ruditapes philippinarum*. *Fish Shellfish Immunol.* 2018;81:502-8.
- Wei S, Huang Y, Cai J, Huang X, Fu J, Qin Q. Molecular cloning and characterization of c-type lysozyme gene in orange-spotted grouper, *Epinephelus coioides*. *Fish Shellfish Immunol.* 2012;33:186-96.
- Wei S, Huang Y, Huang X, Cai J, Wei J, Li P, et al. Molecular cloning and characterization of a new G-type lysozyme gene (Ec-lysG) in orange-spotted grouper, *Epinephelus coioides*. *Dev Comp Immunol.* 2014;46:401-12.
- Whang I, Lee Y, Lee S, Oh MJ, Jung SJ, Choi CY, et al. Characterization and expression analysis of a goose-type lysozyme from the rock bream *Oplegnathus fasciatus*, and antimicrobial activity of its recombinant protein. *Fish Shellfish Immunol.* 2011;30:532-42.
- Xie JW, Cheng CH, Ma HL, Feng J, Su YL, Deng YQ, et al. Molecular characterization, expression and antimicrobial activities of a c-type lysozyme from the mud crab, *Scylla paramamosain*. *Dev Comp Immunol.* 2019;98:54-64.
- Xue QG, Schey KL, Volety AK, Chu FLE, La Peyre JF. Purification and characterization of lysozyme from plasma of the eastern oyster (*Crassostrea virginica*). *Comp Biochem Physiol B Biochem Mol Biol.* 2004;139:11-25.
- Yanagisawa Y, Ochi H. Step-fathering in the anemonefish *Amphiprion clarkii*: a removal study. *Anim Behav.* 1986;34:1769-80.
- Ye X, Zhang L, Tian Y, Tan A, Bai J, Li S. Identification and expression analysis of the g-type and c-type lysozymes in grass carp *Ctenopharyngodon idellus*. *Dev Comp Immunol.* 2010;34:501-9.
- Yildiz HY. Plasma lysozyme levels and secondary stress response in rainbow trout, *Oncorhynchus mykiss* (Walbaum) after exposure to Leteux-Meyer mixture. *Turk J Vet Anim Sci.* 2006;30:265-9.
- Yin X, Hu D, Li JF, He Y, Zhu TD, Wu MC. Contribution of disulfide bridges to the thermostability of a type a feruloyl esterase from *Aspergillus usarii*. *PLOS ONE.* 2015;10:e0126864.
- Zhang S, Xu Q, Boscaro E, Du H, Qi Z, Li Y, et al. Characterization and expression analysis of g- and c-type lysozymes in Dabry's sturgeon (*Acipenser dabryanus*). *Fish Shellfish Immunol.* 2018;76:260-5.
- Zhang X, Wu F, Sun M, Wang Q, Wang Y, Yang X. Study on antimicrobial and antiviral activities of lysozyme from marine strain S-12-86 *in vitro*. *Agric Sci China.* 2008;7:112-6.
- Zhang XH, He X, Austin B. *Vibrio harveyi*: a serious pathogen of fish and invertebrates in mariculture. *Mar Life Sci Technol.* 2020;2:231-45.
- Zhao J, Song L, Li C, Zou H, Ni D, Wang W, et al. Molecular cloning of an invertebrate goose-type lysozyme gene from *Chlamys farreri*, and lytic activity of the recombinant protein. *Mol Immunol.* 2007;44:1198-208.
- Zhao L, Sun J, Sun L. The g-type lysozyme of *Scophthalmus maximus* has a broad substrate spectrum and is involved in the immune response against bacterial infection. *Fish Shellfish Immunol.* 2011;30:630-7.